Measurement and Modeling of CO 2 Solubility in Natural and Synthetic Formation Brines for CO 2 Sequestration

ARTICLE *in* ENVIRONMENTAL SCIENCE AND TECHNOLOGY · JANUARY 2015

Impact Factor: 5.33 · DOI: 10.1021/es505550a · Source: PubMed

6 AUTHORS, INCLUDING:

Haining Zhao
Pennsylvania State University
3 PUBLICATIONS **7** CITATIONS

SEE PROFILE

Douglas Allen
Salem State University
31 PUBLICATIONS **831** CITATIONS

SEE PROFILE

Environmental Science & Technology

Article

pubs.acs.org/est

Measurement and Modeling of CO_2 Solubility in Natural and Synthetic Formation Brines for CO_2 Sequestration

Haining Zhao,[†] Robert Dilmore,[§] Douglas E. Allen,[∥] Sheila W. Hedges,[§] Yee Soong,[§] and Serguei N. Lvov*[,†,‡]

[†]John and Willie Leone Family Department of Energy and Mineral Engineering and [‡]Department of Materials Science and Engineering, The Pennsylvania State University, University Park, Pennsylvania 16802, United States

[§]U.S. Department of Energy National Energy Technology, Laboratory 626, Cochrans Mill Road, Pittsburgh, Pennsylvania 15236, United States

[∥]Department of Geological Sciences, Salem State University, Salem, Massachusetts 01970, United States

Supporting Information

ABSTRACT: CO_2 solubility data in the natural formation brine, synthetic formation brine, and synthetic NaCl+$CaCl_2$ brine were collected at the pressures from 100 to 200 bar, temperatures from 323 to 423 K. Experimental results demonstrate that the CO_2 solubility in the synthetic formation brines can be reliably represented by that in the synthetic NaCl +$CaCl_2$ brines. We extended our previously developed model (PSUCO2) to calculate CO_2 solubility in aqueous mixed-salt solution by using the additivity rule of the Setschenow coefficients of the individual ions (Na^+, Ca^{2+}, Mg^{2+}, K^+, Cl^-, and SO_4^{2-}). Comparisons with previously published models against the experimental data reveal a clear improvement of the proposed PSUCO2 model. Additionally, the path of the maximum gradient of the CO_2 solubility contours divides the *P-T* diagram into two distinct regions: in Region I, the CO_2 solubility in the aqueous phase decreases monotonically in response to increased temperature; in region II, the behavior of the CO_2 solubility is the opposite of that in Region I as the temperature increases.

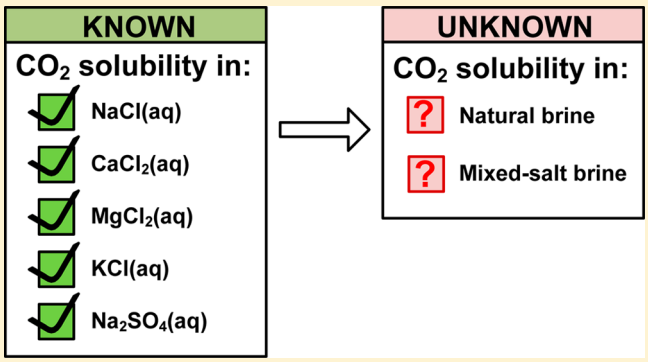

1. INTRODUCTION

Knowledge of the properties of the CO_2-brine system is essential for various energy- and environment-related technical applications, such as CO_2-enhanced oil recovery (CO_2-EOR),[1] CO_2 capture and sequestration (CCS),[2] and CO_2-enhanced geothermal system (CO_2-EGS).[3] The world's first industrial-scale CCS project was initialed at the Sleipner Field in the North Sea since 1996.[2] Although controversy arises between CCS and other low-carbon alternative energy technologies (e.g., wind, nuclear power, solar, biomass, etc.),[4] as well as the widespread use of hydraulic fracturing technologies in shale gas production may break shale layer and cause potential damage of the CO_2 sequestration capacity,[5] the CCS technologies offer a unique opportunity to reduce anthropogenic CO_2 while still allowing the use of fossil fuels.[6] Several large-scale integrated CCS projects are currently operating in the United States and Europe, and more CCS projects have secured financial backing to proceed to construction worldwide.[7] In addition, a CO_2 enhanced geothermal system (CO_2-EGS) has been proposed — utilizing supercritical CO_2 as the heat transmission fluid to extract heat energy from geothermal reservoirs as a means to produce renewable geothermal energy and to concomitantly geologically store CO_2 through potential fluid losses at depth.[3] The CO_2-brine system containing ions of Na^+, Ca^{2+}, Mg^{2+}, K^+, Cl^-, and SO_4^{2-} will be the most commonly encountered fluid system in the above-mentioned engineered natural systems. A good understanding of the CO_2 solubility in aqueous mixed-salt solutions (or natural brine) is, therefore, critical for evaluating, designing, and modeling these industrial processes.[8−10]

In spite of the fact that CO_2 solubility in the CO_2−H_2O system[11,12] and in single-salt aqueous systems[12−16] has been widely studied, investigation of CO_2 solubility in mixed-salt solutions at elevated temperatures and pressures remains few.[17−21] Three previously published models are capable of computing CO_2 solubility in aqueous mixed-salt solutions: the DS2006 model,[22,23] the SP2010 model,[8,11,24] and the OLI Studio 9.0.6 — a commercial software package developed by OLI Systems Inc.[12] All three models show excellent performance in calculating CO_2 solubility in the CO_2−H_2O system and in single-salt systems of CO_2−NaCl−H_2O, CO_2−$CaCl_2$−H_2O, and CO_2−$MgCl_2$−H_2O,[14,15] but their capacity for predicting

Received: November 13, 2014
Revised: January 4, 2015
Accepted: January 5, 2015
Published: January 5, 2015

DOI: 10.1021/es505550a
Environ. Sci. Technol. 2015, 49, 1972−1980

CO_2 solubility in real brines remains to be validated because the experimental data of CO_2 solubility in mixed-salt brine at elevated temperatures and pressures are too scarce to substantiate their performance.

The aim of this study is to provide accurate estimates of CO_2 solubility in natural brines for CO_2 sequestration applications. The three specific objectives are to (1) measure CO_2 solubility in natural brine and in synthetic mixed-salt brines at the *P-T-x* range pertinent to CO_2 sequestration (100 to 200 bar, 323–423 K, ionic strength from 1.7 to 5.0 mol/kg); (2) compare the experimental CO_2 solubility in NaCl+$CaCl_2$ brines with that in synthetic formation brines (seven salt species) at the same pressure, temperature, and ionic strength conditions to find out if a natural brine can be reliably modeled by a simpler proxy brine for CO_2 solubility studies; (3) develop a model to calculate CO_2 solubility in mixed-salt brines and compare the proposed model with previously published models. This paper is organized as follows: Section 2 describes the experimental methods. Section 3 presents the modeling approaches. Both experimental and modeling results are presented in Section 4. In Section 5, we compared the modeling results to the available experimental CO_2 solubility in aqueous mixed-salt solutions. The temperature-dependent behavior of CO_2 solubility in the aqueous phase is also discussed in detail based on the CO_2 solubility contour maps.

2. EXPERIMENTAL METHODS

Chemicals. The carbon dioxide used in all experiments was Coleman Instrument grade with a purity of 99.99%. Water was purified by Milli-Q system and was degassed before loading it into the autoclave. The purified water conductivity was below 6×10^{-6} S/m. All aqueous salt solutions were prepared using this Milli-Q water and ACS grade reagents: sodium chloride (NaCl, J.T. Baker, 99%), calcium chloride ($CaCl_2 \cdot 2H_2O$, Alfa Aesar, 99%), sodium sulfate (Na_2SO_4, Amresco, 99%), magnesium chloride ($MgCl_2$, Alfa Aesar, 99%), potassium chloride (KCl, Alfa Aesar, 99%), strontium chloride ($SrCl_2$, anhydrous, Alfa Aesar, 99%), and sodium bromide (NaBr, Alfa Aesar, 99%).

Synthetic Brine Preparation. The molality based ionic strength ($I = 0.5\ \Sigma_i m_i z_i^2$) was used as a measure of the concentration of aqueous mixed-salt solutions. The brines used for the CO_2 solubility measurements include the following:

(1) a natural Mt. Simon brine with I = 1.815 mol/kg;

(2) a synthetic Mt. Simon formation brine with I = 1.712 mol/kg;

(3) a synthetic NaCl+$CaCl_2$ brine with I = 1.712 mol/kg;

(4) a synthetic Antrim Shale formation brine[25] with I = 4.984 mol/kg;

(5) a synthetic NaCl+$CaCl_2$ brine with I = 4.984 mol/kg.

The chemical compositions of these brines used for the experimental studies are listed in Tables 1 and 2.

Apparatus and Procedure. Because the experimental CO_2 solubility data reported herein were collected at two different laboratories [PSU Energy Institute and National Energy Technology Laboratory (NETL)] independently, there are two different methods employed to measure the CO_2 solubility in the synthetic brines and in the natural Mt. Simon brine. **Method 1** (used by PSU Energy Institute): the experimental system consisted of a 600 mL stainless steel autoclave (Parr Instrument Co.), a 40 mL stainless steel sample cell, a liquid CO_2 pump, and a 300 mL stainless steel pressure cell for sample analysis. After sampling, the dissolved CO_2 in a 40 mL sample cell was slowly released to a 300 mL pressure cell. The mass of the dissolved CO_2 was determined by the pressure and temperature change of the pressure cell before and after CO_2 expansion. The reliability of the experimental technique of Method 1 is confirmed in previous publications.[14,15] Details on the CO_2 solubility measuring technique of Method 1 and the uncertainty analysis approach can be found in a previous publication.[14] **Method 2** (used by NETL): the experimental

Table 1. Chemical Composition of the Natural Mt. Simon Brine[a]

species	c (mg/L)
barium (Ba^{2+})	0.11 ± 0.17
boron (B^{3+})	1.33 ± 0.0
calcium (Ca^{2+})	6877 ± 40
iron ($Fe^{2+/3+}$)	42 ± 13
magnesium (Mg^{2+})	1267 ± 38
manganese (Mn^{2+})	4.9 ± 0.3
potassium (K^+)	717 ± 54
silicon (Si)	9 ± 12
sodium (Na^+)	23317 ± 881
strontium (Sr^{2+})	165 ± 13
sulfur (S^{2-})	568 ± 25
bromide (Br^-)	246 ± 15
chloride (Cl^-)	51068 ± 4361
iodide (I^-)	2.31 ± 1.8
sulfate (SO_4^{2-})	1511 ± 88
I (mol/kg H_2O)	1.815 ± 0.087

[a]Metals were determined by inductively coupled plasma optical emission spectrometry; anions were determined by ion chromatography. The density of the Mt. Simon brine measured at 293 K and 1.013 bar is 1.056 g/cm^3. The total ionic strength (I) is defined by $I = \Sigma_{i=1}^{n} m_i z_i^2$, where m_i and z_i are the molality and charge number of the corresponding ion. I is calculated by converting concentration scale from molarity to molality based on the measured ion concentration listed in Table 1.

Table 2. Chemical Compositions of the Synthetic Mt. Simon Brine and Antrim Shale Formation Brines

	synthetic Mt. Simon formation brine (mol/kg H_2O)		synthetic Antrim Shale formation brine (mol/kg H_2O)	
salt species	proxy brine 1[a]	proxy brine 2[b]	proxy brine 1[a]	proxy brine 2[b]
NaCl	1.0601	1.0601	2.9856	2.9856
$CaCl_2$	0.1365	0.2172	0.3937	0.6661
Na_2SO_4	0.0165		0.0001	
$MgCl_2$	0.0544		0.2535	
KCl	0.0188		0.0222	
$SrCl_2$	0.0021		0.0083	
NaBr	0.0042		0.0090	
I	1.712		4.984	

[a]The synthetic formation brines and the corresponding synthetic NaCl+$CaCl_2$ brines have the same ionic strength. During the PSUCO2 model calculation, the synthetic formation brine composed of seven salt species was simplified to five salt species because the PSUCO2 model is not able to deal with salt species $SrCl_2$ and NaBr. The amount of $SrCl_2$ and NaBr in synthetic formation brines are converted to the equivalent amount of NaCl based on the ionic strength; the concentration of the other salt species remains the same. [b]The proxy NaCl+$CaCl_2$ brine (proxy brine 2) has the same amount of NaCl as the corresponding synthetic formation brine, the concentrations of the other salt species in synthetic formation brines (proxy brine 1) are converted to the equivalent amount of $CaCl_2$ based on the ionic strength.

DOI: 10.1021/es505550a
Environ. Sci. Technol. 2015, 49, 1972–1980

system contains a flexible gold cell hydrothermal rocking autoclave reactor for gas−liquid equilibration. Fluid samples were withdrawn directly into glass, gastight syringes containing a small quantity of 45% (w/w) KOH, which prevents the loss of CO_2 during sampling and analysis. After sampling, KOH-stabilized samples were injected into the acidification module of a UIC coulometric carbon analyzer and titrated using a perchloric acid solution, and the evolved CO_2 was transferred via inert gas stream into a coupled coulometric CO_2 titration cell. The UIC coulometric carbon analyzer is capable of detecting carbon in the range of 0.01 μg to 100 mg; the detailed experimental procedure can be found in Dilmore et al.[26]

3. MODELING

Phase Equilibria Calculation. We use the fugacity-activity approach to calculate fluid phase equilibria for the CO_2−H_2O and CO_2−single salt−H_2O systems — fugacity coefficients of CO_2 and H_2O in the CO_2-rich phase were calculated by a modified Redlich−Kwong EoS,[11,14] and activity coefficients of all components in the aqueous phase were calculated using the Pitzer activity model.[14] The essential Pitzer activity equations and parameters were provided in the Supporting Information; the detailed phase equilibria calculation procedure can be found in Zhao et al.[14] Based on the previous calculation of CO_2 solubility in each CO_2−single salt−H_2O system (single salt refers to NaCl, $CaCl_2$, Na_2SO_4, $MgCl_2$, or KCl),[14,15] we use the additivity rule of Setschenow coefficients of the individual ions to predict the CO_2 solubility in aqueous mixed-salt solutions. Also, we provide a link for the Web-based computational interface of the proposed PSUCO2 model in the Supporting Information.

Additivity Rule of Setschenow Coefficients of the Individual Ions. The salting-out effects of a salt mixture with two or more salt species on a nonelectrolyte have been shown to be accurately additive at ambient conditions[27]

$$\log_{10} C_{CO_2} = \log_{10} C^o_{CO_2} - \sum_{i=1}^{n} N_s^i K_s^i C_t \tag{1}$$

where C_{CO_2} and $C^o_{CO_2}$ are, respectively, the CO_2 molarity (mole per liter of solution) in aqueous mixed-salt solution and in the CO_2−H_2O system at the same temperature and pressure. Note that it is incorrect to use CO_2 molality instead of molarity in eq 1. N_i is the fraction of the i-th salt species defined by $N_i = C_s^i/C_t$, with $C_t = \Sigma_{i=1}^n C_s^i$, where C_s^i and C_t are the molarity of the i-th salt species and the total molar concentration of all dissolved salts, respectively. K_s^i in eq 1 is the Setschenow coefficient for the CO_2 solubility in a single-salt aqueous solution. K_s^i can be evaluated by the classical Setschenow equation[28] as below

$$K_s^i = \frac{1}{C_s^i}\log_{10}\left(\frac{C^o_{CO_2}}{C^i_{CO_2}}\right) \tag{2}$$

where $C^o_{CO_2}$ is the CO_2 molarity in the CO_2−H_2O system, and $C^i_{CO_2}$ is the CO_2 molarity in the single-salt aqueous solution with i-th salt species. In order to evaluate K_s^i, the model calculated CO_2 solubility (in molality) should be converted to CO_2 molarity (C_{CO_2}) using eq 3

$$C^i_{CO_2} = \frac{1000 m^i_{CO_2} \rho^i_{brine}}{1000 + m_s^i Mw_s^i} \tag{3}$$

where $m^i_{CO_2}$ is CO_2 molality in the single-salt aqueous solution with i-th salt species; ρ^i_{brine} is the density (g/cm^3) of the single-salt brine with i-th salt species (Supporting Information); and m_s^i and Mw_s^i are the molality and molecular weight of i-th salt species, respectively. For the CO_2−H_2O system, we treat CO_2 molality ($m^o_{CO_2}$) and CO_2 molarity ($C^o_{CO_2}$) as the same by neglecting the aqueous phase density change due to the dissolution of CO_2. The Setschenow coefficient of a given salt species may be separated by the contribution of individual ions as below[29]

$$K_s^i = \nu^+ K^{i,c}_{s,ion} + \nu^- K^{i,a}_{s,ion} \tag{4}$$

where $K^{i,c}_{s,ion}$ and $K^{i,a}_{s,ion}$ are the separated Setschenow coefficients for cation and anion of the i-th salt species; and ν^+ and ν^- are the stoichiometric coefficients of the corresponding cation and anion, respectively. In PSUCO2, an aqueous mixed-salt solution is treated as the mixture of the six types of ions (Na^+, Ca^{2+}, Mg^{2+}, K^+, Cl^-, and SO_4^{2-}) and H_2O molecules. Other ions in natural brine, such as Ba^{2+}, Sr^{2+}, Fe^{3+}, and Br^-, were neglected during the calculation due to their typically low concentrations in natural solutions. Therefore, for brine with a salt mixture of NaCl, $CaCl_2$, Na_2SO_4, $MgCl_2$, and KCl, eq 4 can be rewritten as below:

$$\begin{aligned}
K_s^{NaCl} &= K^{Na^+}_{s,ion} + K^{Cl^-}_{s,ion}\\
K_s^{CaCl_2} &= K^{Ca^{2+}}_{s,ion} + 2K^{Cl^-}_{s,ion}\\
K_s^{Na_2SO_4} &= 2K^{Na^+}_{s,ion} + K^{SO_4^{2-}}_{s,ion}\\
K_s^{MgCl_2} &= K^{Mg^{2+}}_{s,ion} + 2K^{Cl^-}_{s,ion}\\
K_s^{KCl} &= K^{K^+}_{s,ion} + K^{Cl^-}_{s,ion}\\
K^{Cl^-}_{s,ion} &= 0
\end{aligned} \tag{5}$$

In eq 5, the Cl^- was chosen as a reference ion by assigning $K_s^{Cl^-}$ equals zero. The selection of a reference ion in eq 5 is an arbitrary convention, any other conventions (e.g., $K^{K^+}_{s,ion} = K^{Cl^-}_{s,ion}$ or $K^{SO_4^{2-}}_{s,ion} = 0$, etc.) would be equally good. Given that the Setschenow coefficient (K_s^i) for each single-salt solution is known by eq 2, the Setschenow coefficients for the individual ions ($K_s^{Na^+}$, $K_s^{Ca^{2+}}$, $K_s^{Mg^{2+}}$, $K_s^{K^+}$, and $K_s^{SO_4^{2-}}$) can be computed by solving the set of linear equations (eq 5). The Setschenow coefficient (K_s^{Mix}) due to the addition of mixed salts in aqueous solutions can be calculated using the additivity rule for individual ions as below

$$K_s^{Mix} = \sum_{i=1}^{n} N^i_{s,ion} K^i_{s,ion} \tag{6}$$

where K_s^{Mix} is the Setschenow coefficient of a salt mixture; $N^i_{s,ion}$ is the fraction of the i-th ion defined by $N^i_{s,ion} = C^i_{s,ion}/C_{t,ion}$ and $C_{t,ion} = \Sigma_{i=1}^n C^i_{s,ion}$, where $C^i_{s,ion}$ is the molar concentration of the i-th ion, and $C_{t,ion}$ is the sum of the molar concentration of all ions dissolved in the solution. Once K_s^{Mix} is obtained, the CO_2 molarity in a real brine can be calculated by eq 7 as below:

$$\log_{10} C_{CO_2} = \log_{10} C^o_{CO_2} - K_s^{Mix} C_{t,ion} \tag{7}$$

DOI: 10.1021/es505550a
Environ. Sci. Technol. 2015, 49, 1972−1980

Table 3. Experimental CO_2 Solubility Results in the Synthetic Formation and NaCl+$CaCl_2$ Brines[a]

		method 1							
		I = 1.712 (mol/kg H_2O) synthetic Mt. Simon formation brine				I = 4.984 (mol/kg H_2O) synthetic Antrim Shale formation brine			
		proxy brine 1		proxy brine 2		proxy brine 1		proxy brine 2	
T/K	P/bar	m_{CO2} (mol/kg)	err (mol/kg)	m_{CO_2} (mol/kg)	err (mol/kg)	m_{CO_2} (mol/kg)	err (mol/kg)	m_{CO_2} (mol/kg)	err (mol/kg)
323	100	0.843	0.013	0.850	0.015	0.535	0.015	0.539	0.028
323	125	0.902	0.014	0.898	0.021	0.573	0.014	0.578	0.010
323	150	0.931	0.012	0.925	0.017	0.604	0.014	0.600	0.012
323	175	0.956	0.012	0.951	0.022	0.605	0.008	0.608	0.009
373	100	0.595	0.007	0.590	0.012	0.376	0.011	0.386	0.006
373	125	0.696	0.009	0.691	0.012	0.433	0.004	0.438	0.008
373	150	0.756	0.010	0.759	0.014	0.483	0.010	0.490	0.015
373	175	0.812	0.013	0.818	0.008	0.506	0.010	0.521	0.011
423	100	0.506	0.010	0.505	0.007	0.326	0.013	0.328	0.008
423	125	0.616	0.013	0.608	0.016	0.394	0.026	0.397	0.011
423	150	0.697	0.012	0.703	0.014	0.446	0.004	0.444	0.019
423	175	0.777	0.023	0.780	0.028	0.484	0.010	0.489	0.019

		method 2	
		I = 1.815 (mol/kg H_2O)	
		natural Mt. Simon formation brine	
T/K	P/bar	m_{CO_2} (mol/kg)	err (mol/kg)
328	50.5	0.488	0.030
328	99.8	0.785	0.036
328	150.4	0.849	0.026
328	200.7	0.927	0.011

[a]The instrumental error of Method 1 is about 0.7%. The chemical compositions of synthetic formation brines are listed in Table 2. The chemical compositions of the natural Mt. Simon brine are listed in Table 1.

For given brine composed of the five most frequently encountered salt species (NaCl, $CaCl_2$, Na_2SO_4, $MgCl_2$, and KCl), the calculated results from eq 7 and eq 1 are the same. The difference between these two equations is that the calculation made by eq 1 is based on salt molarity, whereas eq 7 is based on ion molarity. The concentration of natural brine is usually reported by ion molarity (mol/L), thus eq 7 provides a more realistic way to input brine concentration during calculation process. Equation 7 calculated CO_2 molarity (C_{CO_2}) can be converted to CO_2 molality (m_{CO_2}) as below

$$m_{CO_2} = \left(\frac{1000 + TDS}{1000\rho_{brine}^{TDS}}\right) C_{CO_2} \quad (8)$$

where TDS denotes the total dissolved solids (g/L) in the aqueous phase, defined by $TDS = \sum_{i=1}^{n} C_s^i M w_s^i$; and ρ_{brine} is the brine density, which can be calculated by the empirical correlation of ρ_{brine} and TDS (Supporting Information).

4. RESULTS

Experimental CO_2 solubility data in synthetic formation brines (proxy brine 1), synthetic binary NaCl+$CaCl_2$ brines (proxy brine 2), and the natural Mt. Simon brine are listed in Table 3. A natural brine may cause more uncertainties than a synthetic brine for CO_2 solubility measurements because the pH and composition of natural brine may change during the sampling and storage processes; this variation in natural brine may cause uncertainty on CO_2 solubility measurements. In Figure 1a, the experimental CO_2 solubility in natural Mt. Simon brine collected by Method 2 were on average 4.5% lower than the predicted values of the PSUCO2 model, but this difference is considered within the uncertainties of the model calculations (Section 5, Table 5). In addition, Figure 1a shows that the experimental data collected using Method 2 are in good agreement with previously published models (DS2006, SP2010, and OLI Studio 9.0.6). Therefore, Method 2 is considered reliable for measuring CO_2 solubility in brine at the P-T-x conditions pertinent to geologic CO_2 sequestration.

Sodium chloride (NaCl) is the dominant component of natural formation brines, and, therefore, for CO_2 solubility studies, the single-salt aqueous NaCl solution is widely used as a proxy for natural formation brine. Figure 1(b, c) shows the experimental CO_2 solubility in synthetic NaCl+$CaCl_2$ brines is completely overlapped on that in synthetic formation brines at all experimental P-T-x conditions. The experimental results corroborate that NaCl+$CaCl_2$ brine can also be used as a proxy for studying CO_2 solubility in synthetic (or natural) formation brines, provided that the NaCl molality and the total ionic strength are the same for both brines. Additionally, in order to identify a more realistic surrogate between NaCl+$CaCl_2$ and NaCl-only brines for studying CO_2 solubility in natural formation brines, a comparison of the experimental CO_2 solubility between the two brines (NaCl+$CaCl_2$ and NaCl-only) with the same pressure, temperature, and ionic strength is needed.

In this study, we use the modeling results in place of the experimental CO_2 solubility in aqueous NaCl-only solutions to save effort and time from additional experimental work for the CO_2−NaCl−H_2O system, because (1) the CO_2 solubility in aqueous NaCl solution is well-understood at the P-T-x conditions of interest,[14] it can be accurately calculated by either previously published models (DS2006, AD2010,[13] SP2010, and OLI Studio 9.0) or the PSUCO2 model, and (2) the PSUCO2 calculated CO_2 solubility in single salt

DOI: 10.1021/es505550a
Environ. Sci. Technol. 2015, 49, 1972−1980

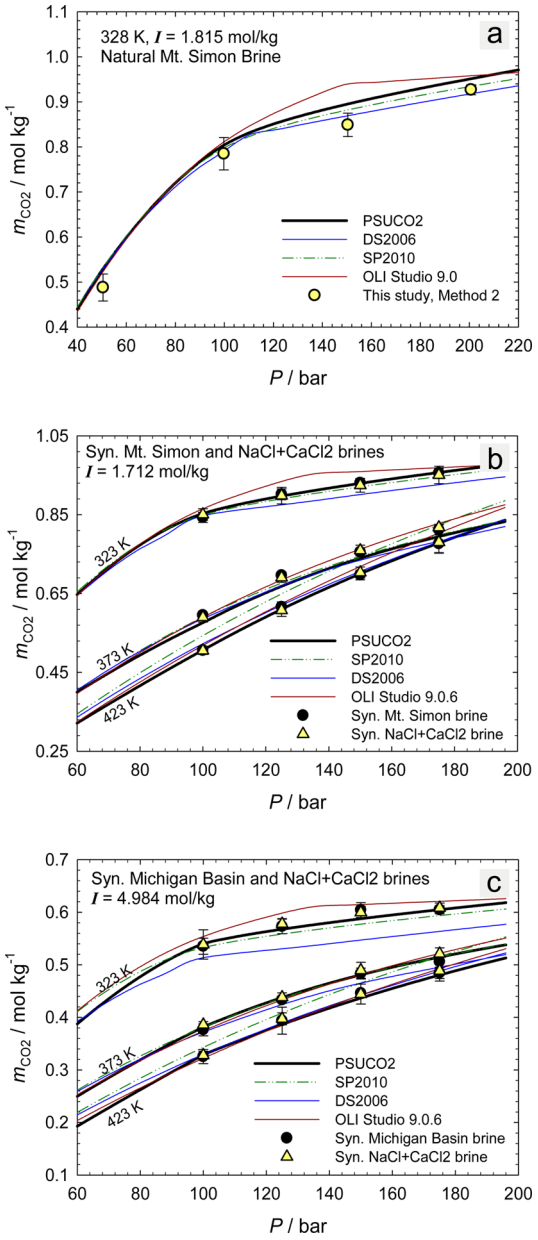

Figure 1. (a-c). Comparison of model calculations (PSUCO2, DS2006, SP2010, and OLI Studio 9.0) with experimental CO_2 solubility measured in this study. (a) Experimental data measured by Method 2. (b, c) Experimental data measured by Method 1. (b) I = 1.712 mol/kg; (c) I = 4.984 mol/kg. For experimental data measured by Method 1 with I = 1.712 mol/kg, 1.0644 mol/kg NaCl, 0.1386 mol/kg $CaCl_2$, 0.0165 mol/kg Na_2SO_4, 0.0544 mol/kg $MgCl_2$, and 0.0188 mol/kg KCl were used as input for each model during calculation processes; for the case of I = 4.984 mol/kg, 2.9946 mol/kg NaCl, 0.4019 mol/kg $CaCl_2$, 0.0001 mol/kg Na_2SO_4, 0.2535 mol/kg $MgCl_2$, and 0.0222 mol/kg KCl were used for the same purpose. For the experimental data collected by Method 2, 1.0547 mol/kg NaCl, 0.1771 mol/kg $CaCl_2$, 0.0162 mol/kg Na_2SO_4, 0.0538 mol/kg $MgCl_2$, and 0.0189 mol/kg KCl (I = 1.815 mol/kg) were used as model inputs during the calculations.

aqueous NaCl solutions (Column 4, Table 4) provides comparable accuracy [average absolute deviation (AAD)<1%] to the corresponding experimental data in aqueous NaCl solutions at 323−423 K, 100−175 bar, and 0−6 mol/kg NaCl.[14]

The overall AAD of the experimental CO_2 solubility in NaCl +$CaCl_2$ brine (Column 5, Table 4) and the PSUCO2 modeling results in NaCl-only brine (Column 4, Table 4) from the experimental CO_2 solubility data in the synthetic formation brines are 0.91% and 2.31%, respectively. Also, the PSUCO2 calculated CO_2 solubility in five-salt brine shows a smaller AAD than that in the NaCl-only brine (Table 4). This comparison shows that the NaCl+$CaCl_2$ brine performs better than NaCl-only brine as a surrogate for studying CO_2 solubility in synthetic (or natural) formation brines. Therefore, for geological CO_2 sequestration and CO_2-EGS applications, the synthetic NaCl+$CaCl_2$ brine offers an accurate, accessible, and inexpensive alternative to researchers who may experience difficulty securing and preserving natural brine samples.

5. DISCUSSION

High Temperature and High Ionic Strength Correction. At 423 K and a high brine concentration (I = 4.984 mol/kg), the modeling results from the additivity rule of Setschenow coefficients of the individual ions show a larger error (AAD = 11.72%) when compared to our experimental CO_2 solubility data in the synthetic Antrim Shale formation brine (proxy brine 1, I = 4.984 mol/kg). It is obvious that this large error is caused by high temperature and high ionic strength conditions, and it further leads to an overall larger AAD (6.55%) of the proposed PSUCO2 model relative to other published models (OLI Studio, SP2010, and DS2006), when compared to our experimental data in the synthetic Antrim Shale formation brine at the entire temperature region of 323 to 423 K (Table 5). Therefore, an error correction term was used in the PSUCO2 model to compensate for the calculation error at the ionic strength greater than 3.0 mol/kg and at the temperature range of 373 to 423 K.

$$\delta_{(m_{CO_2})} = a_1 + \frac{a_2}{T - \Theta} + a_3 I^{0.5} + 10^{-3} a_4 T + a_5 m_{CO_2}$$
$$(373\ \text{K} \le T \le 423\ \text{K and}\ I > 3.0\ \text{mol/kg}) \quad (9)$$
$$\delta_{(m_{CO_2})} = 0\ (\text{other } P\text{-}T\text{-}x \text{ region})$$

The form of eq 9 is the same as the expression of Setchenow coefficients proposed by Akinfiev and Diamond.[13] In eq 9, I is the total ionic strength (mol/kg) of the brine, Θ is a constant and is equal to 228 according to Akinfiev and Diamond.[13] T is temperature in K, and m_{CO_2} is the computed CO_2 molality without correction [eq 8]. The parameters a_1 to a_5 (Table S5, Supporting Information) were determined by the least-squares fitting of eq 9 to the errors between the experimental CO_2 solubility data (this study and the literature data[17,18,21]) and eq 8 calculated values. As a result, the CO_2 solubility (m_{CO_2}) in the mixed-salt solutions at the corresponding temperature and ionic strength conditions can be obtained by adding a correction term (δm_{CO_2}) to m_{CO_2} as below

$$m'_{CO_2} = m_{CO_2} + \delta_{m_{CO_2}} \quad (10)$$

In Table 5, a comparison between the calculated results with and without error correction shows the correction term (δm_{CO_2}) greatly improved the model performance at high temperature and high ionic strength conditions.

Comparison of Different Models against the Literature Data. In Table 5, we presented a comparison of different models (PSUCO2, SP2010, DS2006, and OLI Studio 9.0.6)

DOI: 10.1021/es505550a
Environ. Sci. Technol. 2015, 49, 1972−1980

Table 4. Evaluation of Different Brines As a Surrogate for Studying CO_2 Solubility in Synthetic Formation Brines

		AAD (%)		
proxy brine 1	T/K	1. PSUCO2[a] (NaCl +$CaCl_2$+$MgCl_2$+Na_2SO_4+KCl)	2. PSUCO2[b] (NaCl-only)	3. proxy brine 2 (NaCl+$CaCl_2$)[c]
synthetic Mt. Simon formation brine, I = 1.712 mol/kg, 100−175 bar	323	0.57	3.34	0.61
	373	2.34	1.29	0.67
	423	0.59	0.98	0.69
synthetic Antrim Shale formation brine, I = 4.984 mol/kg, 100−175 bar	323	1.41	6.43	0.69
	373	2.58	0.65	2.05
	423	1.38	1.14	0.71
overall AAD (%)		**1.48**	**2.31**	**0.91**

[a]During the calculation: for I = 1.712 mol/kg, 1.0644 mol/kg NaCl, 0.1386 mol/kg $CaCl_2$, 0.0165 mol/kg Na_2SO_4, 0.0544 mol/kg $MgCl_2$, and 0.0188 mol/kg KCl were used to simulate the proxy brine 1; and for I = 4.984 mol/kg, 2.9946 mol/kg NaCl, 0.4019 mol/kg $CaCl_2$, 0.0001 mol/kg Na_2SO_4, 0.2535 mol/kg $MgCl_2$, and 0.0222 mol/kg KCl were used for the same purpose. [b]The PSUCO2 calculated CO_2 solubility data in aqueous NaCl solution provides a comparable accuracy with the corresponding experimental data.[14] [c]The AAD in this column is calculated between the experimental CO_2 solubility in NaCl+$CaCl_2$ and in synthetic formation brines.

Table 5. Absolute Average Deviations (AAD %) of Model Calculations from the Experimental Data

						model calculations, AAD (%)[b]				
ref	systems	P/ bar	T/K	I/mol/kg	N[a]	PSUCO2 (with error correction)[c]	PSUCO2 (without error correction)[d]	SP2010	DS2006	OLI Studio 9.0.6
19[e]	CO_2−seawater	1−45.6	273−298	0.73	37	8.52 (37)	8.51 (37)	12.46 (24)	13.09 (31)	9.48(37)
20	CO_2−KCl-$CaCl_2$−H_2O	1.013	298	0.4−9.1	54	2.05 (54)	2.05(54)	8.66 (47)	8.26 (51)	3.84 (54)
	CO_2−NaCl-Na_2SO_4−H_2O									
	CO_2−NaCl-KCl-H_2O									
	CO_2−KCl-NaCl-$CaCl_2$−H_2O									
21[f]	CO_2−Weyburn formation brine	17.6−208.7	332	1.58	6	7.39 (6)	7.39 (6)	7.74 (6)	7.75 (6)	7.45 (6)
17	CO_2−NaCl-$CaCl_2$−H_2O	13−160	308−328	1.0−3.2	99	5.52 (99)	7.09 (99)	8.98 (99)	10.87 (99)	5.40 (99)
	CO_2−$CaCl_2$−KCl-H_2O									
	CO_2−KCl-NaCl-H_2O									
	CO_2−NaCl-$CaCl_2$−KCl-H_2O									
18	CO_2−NaCl-KCl-H_2O	10.7−171.6	309−425	1.05	14	4.50 (14)	4.75 (14)	5.91 (14)	5.53 (14)	5.05 (14)
this study[g]	CO_2-Mt. Simon proxy brines 1 and 2	100−175	323−423	1.71	24	1.37 (24)	0.89 (24)	2.92 (24)	2.20 (24)	2.01 (24)
	CO_2-Antrim Shale proxy brines 1 and 2	100−175	323−423	4.98	24	2.07 (24)	6.55 (24)	2.75 (24)	3.69 (24)	1.85 (24)
	CO_2-Mt. Simon brine	50−200	328	1.815	4	4.74 (4)	3.95 (4)	3.84 (4)	3.15 (4)	6.13(4)
overall AAD*						**4.3(225)**	**5.4(225)**	**6.3(218)**	**6.4(222)**	**5.0(225)**

[a]N is the total number of experimental data reported in the literature. [b]The average absolute deviation (AAD) is defined as $AAD(\%) = (100/Np)\Sigma_{i=1}^{N_p}((|m_{CO_2,i}^{calc} - m_{CO_2,i}^{exp})/(m_{CO_2,i}^{exp})|)$ %, where $m_{CO_2,i}^{calc}$ is the model calculated results; $m_{CO_2,i}^{exp}$ is the experimental CO_2 solubility taken from the literature; and N_p represents the total number of experimental data evaluated for each work. [c]"With error correction" means eqs 9 and 10 are used during calculation. [d]"Without error correction" means the calculations were made without using eqs 9 and 10, or δm_{CO_2} always equals zero. [e]The estimates from Stewart and Munjal[18] were not included in the overall AAD due to all the models which significantly deviate from this experimental data. [f]To simulate the Weyburn formation brine, 1.2210 mol/kg NaCl, 0.0505 mol/kg $CaCl_2$, 0.0406 mol/kg Na_2SO_4, 0.0239 mol/kg $MgCl_2$, and 0.0116 mol/kg KCl were used during calculation. The composition of the Weyburn brine is converted from g/cm3 to mol/kg.[21] [g]To simulate the proxy brine 1, for I = 1.712 mol/kg, 1.0644 mol/kg NaCl, 0.1386 mol/kg $CaCl_2$, 0.0165 mol/kg Na_2SO_4, 0.0544 mol/kg $MgCl_2$, and 0.0188 mol/kg KCl were used; and for I = 4.984 mol/kg, 2.9946 mol/kg NaCl, 0.4019 mol/kg $CaCl_2$, 0.0001 mol/kg Na_2SO_4, 0.2535 mol/kg $MgCl_2$, and 0.0222 mol/kg KCl were used during the calculation process.

against the available experimental CO_2 solubility in aqueous mixed-salt solutions. In general, each of the previously published CO_2 solubility model is able to predict the CO_2 solubility in aqueous mixed-salt solutions (or brines) with a

DOI: 10.1021/es505550a
Environ. Sci. Technol. 2015, 49, 1972−1980

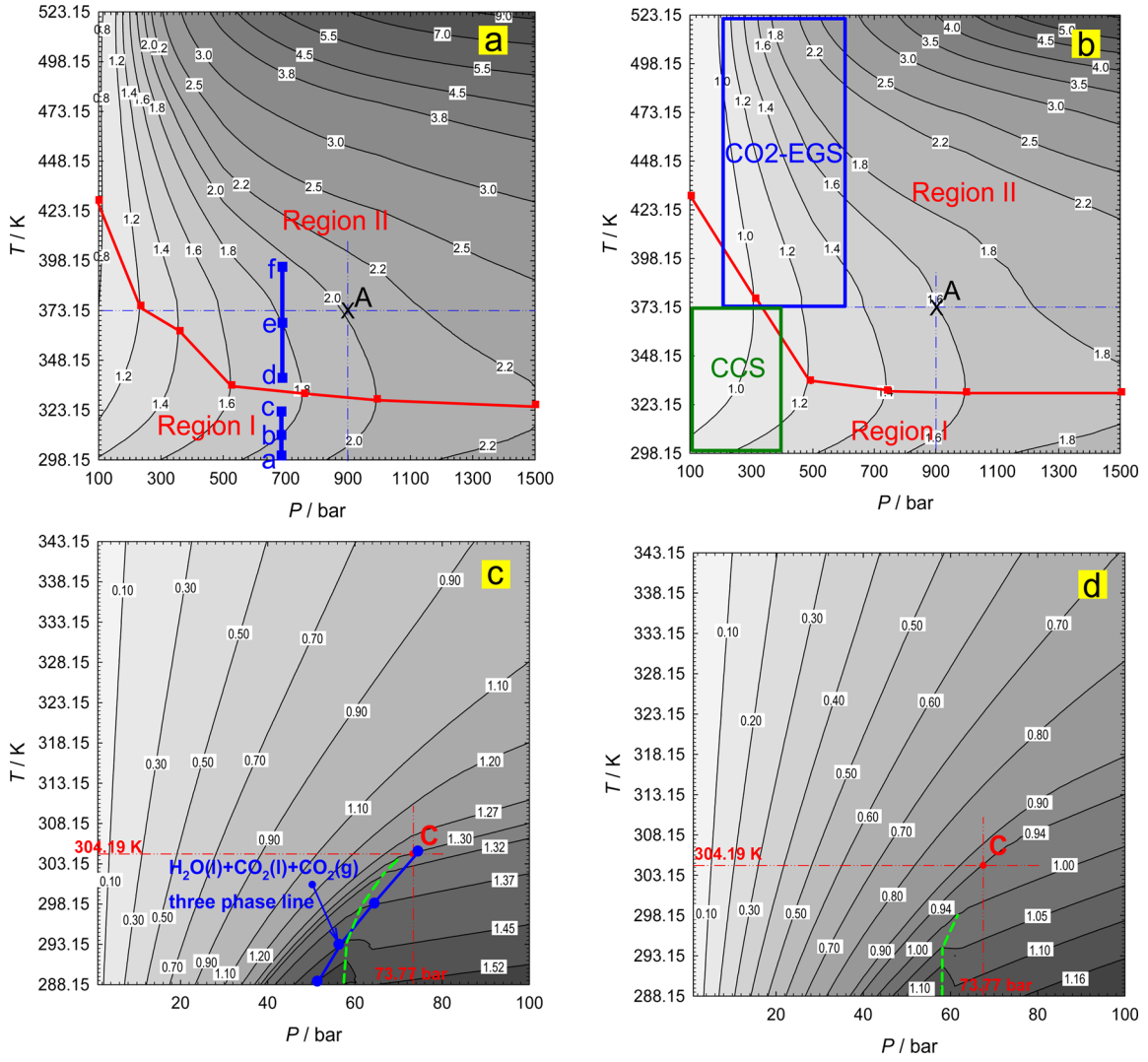

Figure 2. (a-d). The CO_2 solubility contours for the CO_2–H_2O and CO_2–brine systems. Numbers on the contours indicate the CO_2 solubility values by molality (mol/kg): (a) CO_2–H_2O, I = 0 mol/kg, 100–1500 bar, and 298–523 K; (b) synthetic Mt. Simon brine, I = 1.712 mol/kg, 100–1500 bar, and 298–523 K; (c) CO_2–H_2O, I = 0 mol/kg, 1–100 bar, and 288–343 K; (d) synthetic Mt. Simon brine, I = 1.712 mol/kg, 1–100 bar, and 288–343 K. In parts c and d, C is the critical point of CO_2; the blue dot-line represents the experimental three-phase equilibria (CO_2(g)-CO_2(l)-H_2O(l)) measured by Wendland et al.[31] The green dashed lines roughly indicate the start point of discontinuity or wavy behavior of the model calculated contours.

good accuracy (AAD < 6.5%) at the *P-T-x* region of 1 to 200 bar, 288 to 423 K, and ionic strength up to 5 mol/kg (Table 5). However, with the correction term (δm_{CO_2}), the proposed PSUCO2 model takes the smallest overall AAD relative to the other models listed in Table 5.

Although there is a lack of experimental CO_2 solubility to validate the model performance at the pressures higher than 200 bar, the proposed PSUCO2 model can still be safely extended to 600 bar due to the following reasons: (1) the influence of pressure on the additivity rule of Setschenow coefficient is small (AADs are 2.05% at 1 bar, 0.89% at 100–175 bar, Table 5); (2) the model performance for the CO_2–H_2O system and CO_2–single salt–H_2O system are validated by experimental data up to 2000 bar and 573 K.[14,15] Therefore, based on the comparison results listed in Table 5, as well as the reasons listed above, we recommend to use the proposed PSUCO2 model for aqueous mixed-salt solution in the *P-T-x* region of 1 to 600 bar, 288 to 423 K, and ionic strength up to 5 mol/kg. Out of this *P-T-x* region the model can still be used, but the accuracy of the model calculation in aqueous mixed-salt solutions remains untested.

CO_2 Solubility Contour Map. As an application of the proposed PSUCO2 model, the model calculated CO_2 solubility contours on the *P-T* diagram at 100 to 1500 bar and 298 to 523 K for the CO_2–H_2O and CO_2–brine systems are shown in Figure 2(a, b). A clear evidence of the strong salting-out effect on CO_2 solubility in the Mt. Simon formation brine (Figure 2b) can be observed when compared to the CO_2 solubility contours in the CO_2–H_2O system (Figure 2a). Point A on each contour map indicates a fixed *P-T* condition of 900 bar and 373.15 K. The contour for 1.8 mol/kg CO_2 is located on the left side of point A for the CO_2–H_2O system (Figure 2a), when the aqueous phase is changed from water to the Mt. Simon formation brine, the same contour (1.8 mol/kg CO_2) is moved to the right side of point A (Figure 2b).

In addition to the salting-out effect, contour maps Figure 2a and 2b can be divided into two regions (Region I and Region II) based on the temperature-dependent behavior of CO_2

DOI: 10.1021/es505550a
Environ. Sci. Technol. 2015, 49, 1972–1980

solubility in the aqueous phase. The boundary between Region I and Region II is defined as the maximum gradient path between the adjacent CO_2 solubility contours throughout the entire pressure range. In Figure 2(a, b), the path of maximum gradient is roughly shown as the straight lines between the neighbored contours. In Region I, the CO_2 solubility in the aqueous phase decreases monotonically in response to increased temperature, but at a given pressure in region II, the behavior of the CO_2 solubility in response to increased temperature is the opposite of that in Region I. For example, following the isobaric paths *a-b-c* (Region I) and *d-e-f* (Region II) on the *P-T* diagram (Figure 2a), as temperature increases, CO_2 solubility decreases along the path *a-b-c* but increases along the path *d-e-f*. In addition, at points *b* and *e*, CO_2 solubility at two different temperatures but the same pressure reached the same value ($m_{CO_2 lb} = m_{CO_2 le}$ = 1.8 mol/kg). Along the isobaric path *a-b-c-d-e-f*, CO_2 solubility decreases to a minimum and then increases in response to increased temperature. Tutolo et al.[30] also found the similar minimum CO_2 solubility based on their simulation study at the pressures 100, 150, and 200 bar; we have proven this temperature-dependent behavior of CO_2 solubility by defining a "transition zone" on the *P-x* diagram.[14] In this study, the contours on the *P-T* diagram provide an overview on this phenomenon. In Figure 2a, the wavy behavior of the CO_2 solubility contours labeled from 1.2 to 2.2 (with equal step length between labeled values) becomes more and more striking. This trend indicates that (1) an increase in pressure always results in increased CO_2 solubility in the aqueous phase; (2) at a given temperature, the increase of CO_2 solubility in response to increased pressure becomes less notable as pressure increases; (3) at a given pressure within the range from 100 to 1500 bar, the CO_2 solubility always decreases to a minimum and then increases in response to increased temperature; and (4) the temperature corresponding to the minimum CO_2 solubility decreases with increasing pressure.

We also found that the *P-T* region (100−400 bar, 298−373 K)[8] for typical CCS application is located mainly in Region I, whereas the *P-T* window (200−600 bar, 373−573 K)[8] for the CO_2-EGS concept is to be found mainly in Region II, as shown in Figure 2b. Understanding the different temperature-dependent behavior of CO_2 solubility in these two distinct regions may shed light on future work for evaluating and modeling the CCS and CO_2-EGS processes.

Additionally, the hydrostatic (or pore) pressure may be lower than 100 bar for the CO_2-EOR and CCS operations in shallow depleted oil reservoirs. Therefore, in Figures 2c and 2d, we extended the CO_2 solubility contours in Region I to the pressures below 100 bar. In these figures, the contours located in the *P-T* region above or far-away from the CO_2 critical point are smooth, but these below and close to the CO_2 critical point display strong wavy behavior. In order to explain this strange behavior, the three-phase equilibria [CO_2(g)+CO_2(l)+H_2O(l)] experimental data[31] for the CO_2−H_2O system at the *P-T* region of 51.3 to 74.11 bar and 288.67 to 304.63 K are shown in Figure 2c (blue dot-line), and it is a clear evidence that the strange behavior is caused by the occurrence of a new liquid CO_2 phase in the CO_2−H_2O system.

In conclusion, from this study we found that (1) the experimental CO_2 solubility in synthetic NaCl+$CaCl_2$ brines and in synthetic formation brines (Table 3) shows that the NaCl+$CaCl_2$ brine provides a comparable accuracy (AAD < 1%, which is within experimental uncertainties) for studying CO_2 solubility in synthetic (or natural) formation brines; (2) the additivity rule of Setschenow coefficients of the individual ions is proven to be successful in predicting CO_2 solubility in aqueous mixed salt solutions; (3) the proposed PSUCO2 model demonstrates an improvement (Table 5) relative to the previously published models (DS2006, SP2010, and OLI Studio 9.0.6) in predicting CO_2 solubility in formation brines at the *P-T-x* region of 1 to 200 bar, 288 to 423 K, and ionic strength up to 5 mol/kg; and (4) the temperature-dependent behaviors of CO_2 solubility are opposite in the two distinct *P-T* regions at the pressures from 100 to 1500 bar and the temperatures from 298 to 523 K (Figures 2a and 2b).

■ ASSOCIATED CONTENT

Supporting Information

(1) A link for the Internet based computational tool of the proposed CO_2 solubility model; (2) additional model equations and parameters; (3) detailed description of model components; (4) detailed data fitting process for eq 9; (5) brine density correlation; and (6) example of calculated values of the Setschenow coefficient. This material is available free of charge via the Internet at http://pubs.acs.org.

■ AUTHOR INFORMATION

Corresponding Author

*Phone: 814-863-8377. E-mail: lvov@psu.edu. Corresponding author address: 207 Hosler Building, The Pennsylvania State University, University Park.

Notes

The authors declare no competing financial interest.

■ ACKNOWLEDGMENTS

This work was jointly supported by (1) the National Energy Technology Laboratory and the Regional University Alliance (NETL-RUA), the U.S. Department of Energy and (2) the EMS Energy Institute, the Pennsylvania State University, University Park. We thank Dr. Daniel E. Giammar and three anonymous reviewers for carefully reading the manuscript and providing many constructive suggestions and also Dr. Nicolas Spycher and OLI System Inc. for providing us their computer code and software (OLI Studio 9.0.6). This project was funded in part by the Department of Energy, National Energy Technology Laboratory, an agency of the United States Government, through a support contract with URS Energy & Construction, Inc. Neither the United States Government nor any agency thereof, nor any of their employees, nor URS Energy & Construction, Inc., nor any of their employees, makes any warranty, expressed or implied, or assumes any legal liability or responsibility for the accuracy, completeness, or usefulness of any information, apparatus, product, or process disclosed, or represents that its use would not infringe privately owned rights. Reference herein to any specific commercial product, process, or service by trade name, trademark, manufacturer, or otherwise, does not necessarily constitute or imply its endorsement, recommendation, or favoring by the United States Government or any agency thereof. The views and opinions of authors expressed herein do not necessarily state or reflect those of the United States Government or any agency thereof.

DOI: 10.1021/es505550a
Environ. Sci. Technol. 2015, 49, 1972−1980

REFERENCES

(1) Dicharry, R. M.; Perryman, T. L.; Ronquille, J. D. Evaluation and Design of a CO_2 Miscible Flood Project — SACROC Unit, Kelly-Snyder Field. *J. Pet. Technol.* **1973**, *25* (11), 1309−1318.

(2) Eiken, O.; Ringrose, P.; Hermanrud, C.; Nazarian, B.; Torp, T. A.; Høier, L. Lessons learned from 14 years of CCS operations: Sleipner, In Salah and Snøhvit. *Energy Procedia* **2011**, *4*, 5541−5548.

(3) Pruess, K. Enhanced geothermal systems (EGS) using CO_2 as working fluid - A novel approach for generating renewable energy with simultaneous sequestration of carbon. *Geothermics* **2006**, *35* (4), 351−367.

(4) Tsouris, C.; Aaron, D. S.; Williams, K. A. Is carbon capture and storage really needed? *Environ. Sci. Technol.* **2010**, *44* (11), 4042−4045.

(5) Elliot, T. R.; Celia, M. A. Potential restrictions for CO_2 sequestration sites due to shale and tight gas production. *Environ. Sci. Technol.* **2012**, *46* (7), 4223−4227.

(6) Herzog, H. J. What future for carbon capture and sequestration? *Environ. Sci. Technol.* **2001**, *35* (7), 148A−153A.

(7) Echevarria-Huaman, R. N.; Jun, T. X. Energy related CO_2 emissions and the progress on CCS projects: A review. *Renewable Sustainable Energy Rev.* **2014**, *31*, 368−385.

(8) Spycher, N.; Pruess, K. A phase-partitioning model for CO_2-brine mixtures at elevated temperatures and pressures: Application to CO_2-enhanced geothermal systems. *Transp. Porous Med.* **2010**, *82*, 173−196.

(9) Kumar, A.; Noh, M. H.; Ozah, R. C.; Pope, G. A.; Bryant, S. L.; Sepehrnoori, K.; Lake, L. W. Reservoir simulation of CO_2 storage in aquifers. *SPE J.* **2005**, *10* (03), 336−348.

(10) Kampman, N.; Bickle, M.; Wigley, M.; Dubacq, B. Fluid flow and CO_2-fluid-mineral interactions during CO_2-storage in sedimentary basins. *Chem. Geol.* **2014**, *369*, 22−50.

(11) Spycher, N.; Pruess, K.; Ennis-King, J. CO_2-H_2O mixtures in the geological sequestration of CO_2. I. Assessment and calculation of mutual solubilities from 12 to 100 °C and up to 600 bar. *Geochim. Cosmochim. Acta* **2003**, *67* (16), 3015−3031.

(12) Springer, R. D.; Wang, Z.; Anderko, A.; Wang, P.; Felmy, A. R. A thermodynamic model for predicting mineral reactivity in supercritical carbon dioxide: I. Phase behavior of carbon dioxide-water-chloride salt systems across the H_2O-rich to the CO_2-rich regions. *Chem. Geol.* **2012**, *322*−*323* (5), 151−171.

(13) Akinfiev, N. N.; Diamond, L. W. Thermodynamic model of aqueous CO_2-H_2O-NaCl solutions from −22 to 100 °C and from 0.1 to 100 MPa. *Fluid Phase Equilib.* **2010**, *295* (1), 104−124.

(14) Zhao, H.; Fedkin, M. V.; Dilmore, R. M.; Lvov, S. N. Carbon dioxide solubility in aqueous solutions of sodium chloride at geological conditions: Experimental results at 323.15, 373.15, 423.15 K and 150 bar and modeling up to 573.15 K and 2000 bar. *Geochim. Cosmochim. Acta* **2015**, *149*, 165−189.

(15) Zhao, H.; Dilmore, R. M.; Lvov, S. N. Experimental studies and modeling of CO_2 solubility in high temperature aqueous $CaCl_2$, $MgCl_2$, Na_2SO_4, and KCl solutions. *AIChE J.* **2015**, submitted.

(16) Mao, S.; Zhang, D.; Li, Y.; Liu, N. An improved model for calculating CO_2 solubility in aqueous NaCl solutions and the application to CO_2-H_2O-NaCl fluid inclusions. *Chem. Geol.* **2013**, *347*, 43−58.

(17) Liu, Y.; Hou, M.; Yang, G.; Han, B. Solubility of CO_2 in aqueous solutions of NaCl, KCl, $CaCl_2$ and their mixed salts at different temperatures and pressures. *J. Supercrit. Fluids* **2011**, *56* (2), 125−129.

(18) Tong, D.; Martin-Trusler, J. P.; Vega-Maza, D. Solubility of CO_2 in aqueous solutions of $CaCl_2$ or $MgCl_2$ and in a synthetic formation brine at temperatures up to 423 K and pressures up to 40 MPa. *J. Chem. Eng. Data* **2013**, *58* (7), 2116−2124.

(19) Stewart, P. B.; Munjal, P. Solubility of carbon dioxide in pure water, synthetic sea water, and synthetic sea water concentrates at −50 to 250 °C and 10 to 45 atm. pressures. *J. Chem. Eng. Data* **1970**, *15* (1), 67−71.

(20) Yasunishi, A.; Tsuji, M.; Sada, E. Solubility of carbon dioxide in aqeuous mixed-salt solutions. In *Thermodynamic Behavior of Electrolytes in Mixed Solvents-II Advances in Chemistry Series*; Furter, W. F., Eds.; American Chemical Society: Washington, DC, 1979; pp 189−203.

(21) Li, Z.; Dong, M.; Li, S.; Dai, L. Densities and solubilites for binary systems of carbon dioxide+water and carbon dioxide+brine at 59 °C and pressures to 29 MPa. *J. Chem. Eng. Data* **2004**, *49* (4), 1026−1031.

(22) Duan, Z.; Sun, R. An improved model calculating CO_2 solubility in pure water and aqueous NaCl solutions from 273 to 533 K and from 0 to 2000 bar. *Chem. Geol.* **2003**, *193* (3−4), 257−271.

(23) Duan, Z.; Sun, R.; Zhu, C.; Chou, I.-M. An improved model for the calculation of CO_2 solubility in aqueous solutions containing Na^+, K^+, Ca^{2+}, Mg^{2+}, Cl^-, and SO_4^{2-}. *Mar. Chem.* **2006**, *98* (2−4), 131−139.

(24) Spycher, N.; Pruess, K. CO_2-H_2O mixtures in the geological sequestration of CO_2. II. Partitioning in chloride brines at 12−100 °C and up to 600 bar. *Geochim. Cosmochim. Acta* **2005**, *69* (13), 3309−3320.

(25) McIntosh, J. C.; Water, L. M.; Martini, A. M. Extensive microbial modification of formation water geochemistry: Case study from a Midcontinent sedimentary basin, United States. *Geol. Soc. Am. Bull.* **2004**, *116* (5), 743−759.

(26) Dilmore, R. M.; Allen, D. E.; Richard-Mccarthy Jones, J.; Hedges, S. W.; Soong, Y. Sequestration of dissolved CO_2 in the Oriskany Formation. *Environ. Sci. Technol.* **2008**, *42* (8), 2760−2766.

(27) Gordon, J. E.; Thorne, R. L. Salt effects on non-electrolyte activity coefficients in mixed aqueous electrolyte solutions-II. Artificial and natural sea waters. *Geochim. Cosmochim. Acta* **1967**, *31* (12), 2433−2443.

(28) Setschenow, J. Über die Konstitution der Salzlösungen auf Grund ihres Verhaltens zu Kohlensäure. *Z. Phys. Chem.* **1889**, *4*, 117−128.

(29) Görgényi, M.; Dewulf, J.; Van-Langenhove, H.; Héberger, K. Aqueous salting-out effect of inorganic cations and anions on non-electrolytes. *Chemosphere* **2006**, *65* (5), 802−810.

(30) Tutolo, B. M.; Luhmann, A. J.; Kong, X.-Z.; Saar, M. O.; Seyfried, W. E., Jr. Experimental observation of permeability changes in dolomite at CO_2 sequestration conditions. *Environ. Sci. Technol.* **2014**, *48* (4), 2445−2452.

(31) Wendland, M.; Hasse, H.; Maurer, G. Experimental pressure-temperature data on three- and four-phase equilibria of fluid, hydrate, and ice phases in the system carbon dioxide-water. *J. Chem. Eng. Data* **1999**, *44* (5), 901−906.

DOI: 10.1021/es505550a
Environ. Sci. Technol. 2015, 49, 1972−1980